

Lepton flavor conserving Z boson decays and scalar unparticle

E. O. Iltan, *

Physics Department, Middle East Technical University
Ankara, Turkey

Abstract

We predict the contribution of scalar unparticle to the branching ratios of the lepton flavor conserving $Z \rightarrow l^+l^-$ decays and we study the discrepancy between the experimental and the QED corrected standard model branching ratios . We observe that these decays are sensitive to the unparticle scaling dimension d_u for its small values, especially for heavy lepton flavor output.

*E-mail address: eiltan@newton.physics.metu.edu.tr

Theoretically, Z boson decays to lepton pairs exist in the tree level, in the standard model (SM) if the lepton flavor is conserved. The improved experimental measurements stimulate the studies of these interactions and with the Giga-Z option of the Tesla project, there is a possibility to increase Z bosons at resonance [1]. The experimental predictions for the branching ratios (BRs) of these decays are [2]

$$\begin{aligned} BR(Z \rightarrow e^+e^-) &= 3.363 \pm 0.004 \%, \\ BR(Z \rightarrow \mu^+\mu^-) &= 3.366 \pm 0.007 \%, \\ BR(Z \rightarrow \tau^+\tau^-) &= 3.370 \pm 0.0023 \%, \end{aligned} \tag{1}$$

and the tree level SM predictions, including QED corrections read

$$\begin{aligned} BR(Z \rightarrow e^+e^-) &= 3.3346 \%, \\ BR(Z \rightarrow \mu^+\mu^-) &= 3.3346 \%, \\ BR(Z \rightarrow \tau^+\tau^-) &= 3.3338 \%. \end{aligned} \tag{2}$$

It is seen that the main contribution to BRs of Z boson lepton pair decays is coming from the tree level SM contribution and the discrepancy between the experimental and the SM results is of the order of 1.0 %. In the literature, there are various experimental and theoretical studies [3]-[18]. The vector and axial coupling constants in Z-decays have been measured at LEP [8] and various additional types of interactions have been performed. A way to measure these contributions in the process $Z \rightarrow \tau^+\tau^-$ was described in [11]. In [17] and [18] the possible new physics effects to the process $Z \rightarrow l^+l^-$, in the two Higgs doublet model and in the SM with the non-commutative effects have been studied, respectively.

The present work is devoted to analysis whether the inclusion of the scalar unparticle effects overcomes the discrepancy of the BRs between the experimental and the QED corrected SM result (see [19] and references therein) for the lepton flavor conserving (LFC) Z decays. Furthermore, we study the new parameters arising with the unparticle effects and the dependencies of the BRs to these new parameters.

The unparticle idea is introduced by Georgi [20, 21] and its effect in the processes, which are induced at least in one loop level, is studied in various works [22]-[31]. This idea is based on the interaction of the SM and the ultraviolet sector with non-trivial infrared fixed point, at high energy level. The unparticles, being massless and having non integral scaling dimension d_u , are new degrees of freedom arising from the ultraviolet sector around $\Lambda_U \sim 1\text{ TeV}$. The effective lagrangian which is responsible for the interactions of unparticles with the SM fields

in the low energy level reads

$$\mathcal{L}_{eff} \sim \frac{\eta}{\Lambda_U^{d_u+d_{SM}-n}} O_{SM} O_U, \quad (3)$$

where O_U is the unparticle operator, the parameter η is related to the energy scale of ultraviolet sector, the low energy one and the matching coefficient [20, 21, 32] and n is the space-time dimension.

Now, we present the effective lagrangian which drives the $Z \rightarrow l^+ l^-$ decays with internal scalar unparticle mediation. Here, we consider the operators with the lowest possible dimension since they have the most powerful effect in the low energy effective theory (see for example [33]). The low energy effective interaction lagrangian which induces $U - l - l$ vertex is

$$\mathcal{L}_1 = \frac{1}{\Lambda_U^{d_u-1}} (\lambda_{ij}^S \bar{l}_i l_j + \lambda_{ij}^P \bar{l}_i i \gamma_5 l_j) O_U, \quad (4)$$

where l is the lepton field and λ_{ij}^S (λ_{ij}^P) is the scalar (pseudoscalar) coupling. In addition to this lagrangian, the one which causes the tree level $U - Z - Z$ interaction (see Fig 1 (b) and (c)), appearing in the scalar unparticle mediating loop, can exist and it reads

$$\mathcal{L}_2 = \frac{\lambda_0}{\Lambda_U^{d_u}} F_{\mu\nu} F^{\mu\nu} O_U + \frac{\lambda_Z}{\Lambda_U^{d_u}} m_Z^2 Z^\mu Z_\mu O_U, \quad (5)$$

where $F_{\mu\nu}$ is the field tensor for the Z_μ field and λ_0 and λ_Z are effective coupling constants¹.

Since the scalar unparticle contribution $Z \rightarrow l^+ l^-$ decay enters into calculations at least in the one loop level (see Fig.1), one needs the scalar unparticle propagator and it is obtained by using the scale invariance [21, 34]:

$$\int d^4x e^{ipx} \langle 0 | T(O_U(x) O_U(0)) | 0 \rangle = i \frac{A_{d_u}}{2\pi} \int_0^\infty ds \frac{s^{d_u-2}}{p^2 - s + i\epsilon} = i \frac{A_{d_u}}{2 \sin(d_u \pi)} (-p^2 - i\epsilon)^{d_u-2}, \quad (6)$$

where the function $\frac{1}{(-p^2 - i\epsilon)^{2-d_u}}$ reads

$$\frac{1}{(-p^2 - i\epsilon)^{2-d_u}} \rightarrow \frac{e^{-i d_u \pi}}{(p^2)^{2-d_u}}, \quad (7)$$

for $p^2 > 0$ and a non-trivial phase appears as a result of non-integral scaling dimension. Here where the factor A_{d_u} is

$$A_{d_u} = \frac{16 \pi^{5/2}}{(2\pi)^{2d_u}} \frac{\Gamma(d_u + \frac{1}{2})}{\Gamma(d_u - 1) \Gamma(2d_u)}. \quad (8)$$

¹The vertex factor: $\frac{i}{\Lambda_U^{d_u}} m_Z^2 \lambda_Z g_{\mu\nu} + \frac{4i}{\Lambda_U^{d_u}} \lambda_0 (k_{1\nu} k_{2\mu} - k_1 \cdot k_2 g_{\mu\nu})$ where $k_{1(2)}$ is the four momentum of Z boson with polarization vector $\epsilon_{1\mu(2\nu)}$.

At this stage, we are ready to consider the general effective vertex for the interaction of on-shell Z-boson with a fermionic current:

$$\Gamma_\mu = \gamma_\mu (f_V - f_A \gamma_5) + \frac{i}{m_W} (f_M + f_E \gamma_5) \sigma_{\mu\nu} q^\nu, \quad (9)$$

where q is the momentum transfer, $q^2 = (p - p')^2$, f_V (f_A) is vector (axial-vector) coupling, f_M (f_E) is proportional to the weak magnetic (electric dipole) moments of the fermion. Here p ($-p'$) is the four momentum vector of lepton (anti-lepton). The form factors f_V , f_A , f_M and f_E in eq. (9) are obtained as

$$\begin{aligned} f_V &= f_V^{SM} + \int_0^1 dx f_{V self}^U + \int_0^1 dx \int_0^{1-x} dy f_{V vert}^U, \\ f_A &= f_A^{SM} + \int_0^1 dx f_{A self}^U + \int_0^1 dx \int_0^{1-x} dy f_{A vert}^U, \\ f_M &= \int_0^1 dx \int_0^{1-x} dy f_{M vert}^U, \\ f_E &= \int_0^1 dx \int_0^{1-x} dy f_{E vert}^U, \end{aligned} \quad (10)$$

where the QED corrected² SM form factors f_V^{SM} and f_A^{SM} are [19]

$$\begin{aligned} f_V^{SM} &= \frac{-i e}{c_W s_W} (\bar{c}_1 + \bar{c}_2), \\ f_A^{SM} &= \frac{-i e}{c_W s_W} (\bar{c}_2 - \bar{c}_1), \end{aligned} \quad (11)$$

with

$$\begin{aligned} \bar{c}_1 &= c_1 + \frac{3}{16} \left(\frac{\alpha_{EM}}{\pi} (2 s_W^2 - 1) + \frac{4 m_l^2}{m_Z^2} \right), \\ \bar{c}_2 &= c_2 + \frac{3}{8} \left(\frac{\alpha_{EM}}{\pi} s_W^2 - \frac{2 m_l^2}{m_Z^2} \right). \end{aligned} \quad (12)$$

Here the parameters c_1 and c_2 read

$$\begin{aligned} c_1 &= -\frac{1}{2} + s_W^2, \\ c_2 &= s_W^2. \end{aligned} \quad (13)$$

On the other hand the explicit expressions of the form factors $f_{V self}^U$, $f_{A self}^U$, $f_{V vert}^U$, $f_{A vert}^U$, $f_{M vert}^U$ and $f_{E vert}^U$, carrying scalar unparticle effects, are

$$f_{V self}^U = \frac{-i c_{self} (c_1 + c_2) L_{self}^{d_u-1} (1-x)^{2-d_u}}{32 s_W c_W (d_u - 1) \pi^2} \sum_{i=1}^3 \left((\lambda_{il}^S)^2 + (\lambda_{il}^P)^2 \right),$$

²The corrections are taken to the lowest approximation in α_{EM}

$$f_{A self}^U = \frac{i c_{self} (c_2 - c_1) L_{self}^{d_u-1} (1-x)^{2-d_u}}{32 s_W c_W (d_u - 1) \pi^2} \sum_{i=1}^3 \left((\lambda_{il}^S)^2 + (\lambda_{il}^P)^2 \right),$$

$$\begin{aligned} f_{V vert}^U &= \frac{i c_{ver} (c_1 + c_2) (1-x-y)^{1-d_u}}{32 \pi^2} \sum_{i=1}^3 \frac{1}{L_{vert}^{2-d_u}} \left\{ 2 \left((\lambda_{il}^S)^2 - (\lambda_{il}^P)^2 \right) m_i m_l (1-x-y) \right. \\ &+ \left. \left((\lambda_{il}^S)^2 + (\lambda_{il}^P)^2 \right) \left(m_i^2 + m_Z^2 x y + m_l^2 (1-x-y)^2 - \frac{L_{vert}}{1-d_u} \right) \right\} \\ &+ \frac{\lambda_0 m_Z^2}{16 \pi^2} \sum_{i=1}^3 \left\{ \frac{b_{ver} y^{1-d_u}}{L_{1 vert}^{2-d_u}} \left\{ m_i \left((c_1 - c_2) \lambda_{il}^P + i (c_1 + c_2) \lambda_{il}^S \right) (x-y-1) \right. \right. \\ &+ m_l \left((c_1 - c_2) \lambda_{il}^P - i (c_1 + c_2) \lambda_{il}^S \right) \left((x+y)^2 + y-x \right) \Big\} \\ &+ \frac{b'_{ver} x^{1-d_u}}{L_{2 vert}^{2-d_u}} \left\{ m_i \left((c_1 - c_2) \lambda_{il}^P - i (c_1 + c_2) \lambda_{il}^S \right) (x-y+1) \right. \\ &- m_l \left((c_1 - c_2) \lambda_{il}^P + i (c_1 + c_2) \lambda_{il}^S \right) \left((x+y)^2 - y+x \right) \Big\} \Big\} \\ &+ \frac{\lambda_Z}{32 \pi^2} \sum_{i=1}^3 \left\{ \frac{b_{ver} y^{1-d_u}}{L_{1 vert}^{2-d_u}} \left\{ \left((c_1 - c_2) \lambda_{il}^P - i (c_1 + c_2) \lambda_{il}^S \right) \left(m_Z^2 m_l (x y (x+y-1) \right. \right. \right. \\ &+ x+y) - m_l^3 (1-x-y)^2 (x+y) + \frac{L_{1 vert}}{2(d_u-1)} m_l (1+6(x+y-1)) \Big\} \\ &+ \left. \left((c_1 - c_2) \lambda_{il}^P + i (c_1 + c_2) \lambda_{il}^S \right) m_i \left(m_l^2 (1-x-y)^2 - m_Z^2 - \frac{L_{1 vert}}{2(d_u-1)} \right) \right\} \\ &+ \frac{b'_{ver} x^{1-d_u}}{L_{1 vert}^{2-d_u}} \left\{ \left((c_1 - c_2) \lambda_{il}^P + i (c_1 + c_2) \lambda_{il}^S \right) \left(m_l^3 (1-x-y)^2 (x+y) \right. \right. \\ &- m_Z^2 m_l (x y (x+y-1) + x+y) - \frac{L_{2 vert}}{2(d_u-1)} m_l (1+6(x+y-1)) \Big\} \\ &- \left. \left((c_1 - c_2) \lambda_{il}^P - i (c_1 + c_2) \lambda_{il}^S \right) m_i \left(m_l^2 (1-x-y)^2 - m_Z^2 - \frac{L_{2 vert}}{2(d_u-1)} \right) \right\} \Big\}, \end{aligned}$$

$$\begin{aligned} f_{A vert}^U &= \frac{-i c_{ver} (c_1 - c_2) (1-x-y)^{1-d_u}}{32 \pi^2} \sum_{i=1}^3 \frac{1}{L_{vert}^{2-d_u}} \left\{ \left((\lambda_{il}^P)^2 - (\lambda_{il}^S)^2 \right) \left(2 m_i m_l (1-x-y) \right. \right. \\ &- \left. \left((\lambda_{il}^S)^2 + (\lambda_{il}^P)^2 \right) \left(m_i^2 - m_Z^2 x y + m_l^2 (1-x-y)^2 - \frac{L_{vert}}{d_u-1} \right) \right\} \\ &- \frac{\lambda_0 m_Z^2}{16 \pi^2} \sum_{i=1}^3 \left\{ \frac{b_{ver} y^{1-d_u}}{L_{1 vert}^{2-d_u}} \left\{ m_i \left((c_1 + c_2) \lambda_{il}^P + i (c_1 - c_2) \lambda_{il}^S \right) (1-x+y) \right. \right. \\ &- m_l \left((c_1 + c_2) \lambda_{il}^P - i (c_1 - c_2) \lambda_{il}^S \right) \left((x+y) (1-x+y) \right) \Big\} \\ &+ \frac{b'_{ver} x^{1-d_u}}{L_{2 vert}^{2-d_u}} \left\{ m_i \left((c_1 + c_2) \lambda_{il}^P - i (c_1 - c_2) \lambda_{il}^S \right) (y-x-1) \right. \\ &+ m_l \left((c_1 + c_2) \lambda_{il}^P + i (c_1 - c_2) \lambda_{il}^S \right) \left((x+y) (1+x-y) \right) \Big\} \Big\} \end{aligned}$$

$$\begin{aligned}
& + \frac{\lambda_Z}{32\pi^2} \sum_{i=1}^3 \left\{ \frac{b_{ver} y^{1-d_u}}{L_{1vert}^{2-d_u}} \left\{ ((c_1 + c_2) \lambda_{il}^P - i(c_1 - c_2) \lambda_{il}^S) \left(m_Z^2 m_l (x + y) \right. \right. \right. \\
& + \left. \left. \frac{L_{1vert}}{2(d_u - 1)} m_l \right) - ((c_1 + c_2) \lambda_{il}^P + i(c_1 - c_2) \lambda_{il}^S) m_i \left(\frac{L_{1vert}}{2(d_u - 1)} + m_Z^2 \right) \right\} \\
& - \frac{b'_{ver} x^{1-d_u}}{L_{2vert}^{2-d_u}} \left\{ ((c_1 + c_2) \lambda_{il}^P + i(c_1 - c_2) \lambda_{il}^S) \left(m_Z^2 m_l (x + y) \right. \right. \\
& + \left. \left. \frac{L_{2vert}}{2(d_u - 1)} m_l \right) - ((c_1 + c_2) \lambda_{il}^P - i(c_1 - c_2) \lambda_{il}^S) m_i \left(\frac{L_{2vert}}{2(d_u - 1)} + m_Z^2 \right) \right\} \Big\}, \quad (14)
\end{aligned}$$

$$\begin{aligned}
f_{Mvert}^U = & - \frac{i(1-x-y)^{1-d_u}}{32\pi^2} \sum_{i=1}^3 \frac{c_{ver} m_Z c_W}{L_{vert}^{2-d_u}} \left\{ m_i \left(((\lambda_{il}^S)^2 - (\lambda_{il}^P)^2) (c_1 + c_2) (x + y) \right. \right. \\
& - \left. \left. 2i \lambda_{il}^S \lambda_{il}^P (c_2 - c_1) (x - y) \right) + ((\lambda_{il}^S)^2 + (\lambda_{il}^P)^2) (c_1 + c_2) (1 - x - y) (x + y) \right\} \\
& - \frac{i\lambda_0}{8\pi^2} \sum_{i=1}^3 \left\{ \frac{b_{ver} m_Z c_W y^{1-d_u}}{L_{1vert}^{2-d_u}} \left(c_1 (\lambda_{il}^S + i\lambda_{il}^P) + c_2 (\lambda_{il}^S - i\lambda_{il}^P) \right) \left(m_Z^2 x y + \frac{L_{1vert}}{d_u - 1} \right) \right. \\
& + \left. \frac{b'_{ver} m_Z c_W x^{1-d_u}}{L_{2vert}^{2-d_u}} \left(c_1 (\lambda_{il}^S - i\lambda_{il}^P) + c_2 (\lambda_{il}^S + i\lambda_{il}^P) \right) \left(m_Z^2 x y + \frac{L_{2vert}}{d_u - 1} \right) \right\} \\
& - \frac{i\lambda_Z}{64\pi^2} \sum_{i=1}^3 \left\{ \frac{b_{ver} m_Z c_W y^{1-d_u}}{L_{1vert}^{2-d_u}} \left\{ (c_1 + c_2) \lambda_{il}^S \left(-m_i m_l (1 - x - y)^2 \right. \right. \right. \\
& - \left. \left. m_l^2 (1 - x - y)^2 (x + y) + m_Z^2 x (2 - y(1 - x - y)) + (3x + 3y - 2) \frac{L_{1vert}}{d_u - 1} \right) \right. \\
& + \left. i(c_1 - c_2) \lambda_{il}^P \left(m_i m_l (1 - x - y)^2 - m_l^2 (1 - x - y)^2 (x + y) \right. \right. \\
& + \left. \left. m_Z^2 x (2 - y(1 - x - y)) + (3x + 3y - 2) \frac{L_{1vert}}{d_u - 1} \right) \right\} \\
& + \frac{b'_{ver} m_Z c_W x^{1-d_u}}{L_{2vert}^{2-d_u}} \left\{ (c_1 + c_2) \lambda_{il}^S \left(-m_i m_l (1 - x - y)^2 - m_l^2 (1 - x - y)^2 (x + y) \right. \right. \\
& + \left. \left. m_Z^2 y (2 - x(1 - x - y)) + (3x + 3y - 2) \frac{L_{2vert}}{d_u - 1} \right) - i(c_1 - c_2) \lambda_{il}^P \left(m_i m_l (1 - x - y)^2 \right. \right. \\
& - \left. \left. m_l^2 (1 - x - y)^2 (x + y) + m_Z^2 y (2 - x(1 - x - y)) + (3x + 3y - 2) \frac{L_{2vert}}{d_u - 1} \right) \right\} \Big\},
\end{aligned}$$

$$\begin{aligned}
f_{Evert}^U = & - \frac{i(1-x-y)^{1-d_u}}{32\pi^2} \sum_{i=1}^3 \frac{c_{ver} m_Z c_W}{L_{vert}^{2-d_u}} \left\{ m_i \left(((\lambda_{il}^S)^2 - (\lambda_{il}^P)^2) (c_1 - c_2) (x - y) \right. \right. \\
& + \left. \left. 2i \lambda_{il}^S \lambda_{il}^P (c_1 + c_2) (x + y) \right) + m_l \left(((\lambda_{il}^S)^2 + (\lambda_{il}^P)^2) (c_1 - c_2) (1 - x - y) (x - y) \right) \right\} \\
& - \frac{i\lambda_0}{8\pi^2} \sum_{i=1}^3 \left\{ \frac{b_{ver} m_Z c_W y^{1-d_u}}{L_{1vert}^{2-d_u}} \left((c_1 (\lambda_{il}^S + i\lambda_{il}^P) - c_2 (\lambda_{il}^S - i\lambda_{il}^P)) \left(m_Z^2 x y \right. \right. \right. \\
& + \left. \left. m_l^2 (1 - x - y) (x + y) - \frac{L_{1vert}}{1 - d_u} \right) + \left(c_1 (\lambda_{il}^S - i\lambda_{il}^P) - c_2 (\lambda_{il}^S + i\lambda_{il}^P) \right) m_i m_l (1 - x - y) \right) \Big\}
\end{aligned}$$

$$\begin{aligned}
& + \frac{b'_{ver} m_Z c_W x^{1-d_u}}{L_{2vert}^{2-d_u}} \left(\left(c_2 (\lambda_{il}^S + i \lambda_{il}^P) - c_1 (\lambda_{il}^S - i \lambda_{il}^P) \right) \left(m_Z^2 x y + m_l^2 (1-x-y)(x+y) \right. \right. \\
& - \left. \left. \frac{L_{2vert}}{1-d_u} \right) - \left(c_1 (\lambda_{il}^S + i \lambda_{il}^P) - c_2 (\lambda_{il}^S - i \lambda_{il}^P) \right) m_i m_l (1-x-y) \right) \Big\} \\
& - \frac{i \lambda_Z}{64 \pi^2} \sum_{i=1}^3 \left\{ \frac{b_{ver} m_Z c_W y^{1-d_u}}{L_{1vert}^{2-d_u}} \left\{ (i (c_1 + c_2) \lambda_{il}^P \left(m_i m_l (y^2 - (1-x)^2) \right. \right. \right. \\
& + m_l^2 (1-x-y) ((x+y)^2 - x+y) + m_Z^2 x (2-y(1-x-y)) + (3x+3y-2) \frac{L_{1vert}}{d_u-1} \Big) \\
& - (c_1 - c_2) \lambda_{il}^S \left(m_i m_l (y^2 - (1-x)^2) - m_l^2 (1-x-y) ((x+y)^2 - x+y) \right. \\
& - \left. \left. m_Z^2 x (2-y(1-x-y)) - (3x+3y-2) \frac{L_{1vert}}{d_u-1} \right) \right\} \\
& + \frac{b'_{ver} m_Z c_W x^{1-d_u}}{L_{2vert}^{2-d_u}} \left\{ i (c_1 + c_2) \lambda_{il}^P \left(m_i m_l (x^2 - (1-y)^2) \right. \right. \\
& + m_l^2 (1-x-y) ((x+y)^2 - y+x) + m_Z^2 y (2-x(1-x-y)) + (3x+3y-2) \frac{L_{2vert}}{d_u-1} \Big) \\
& + (c_1 - c_2) \lambda_{il}^S \left(m_i m_l (x^2 - (1-y)^2) - m_l^2 (1-x-y) ((x+y)^2 - y+x) \right. \\
& - \left. \left. m_Z^2 x (2-x(1-x-y)) - (3x+3y-2) \frac{L_{2vert}}{d_u-1} \right) \right\} \Big\}, \tag{15}
\end{aligned}$$

with

$$\begin{aligned}
L_{self} &= x \left(m_l^2 (1-x) - m_i^2 \right), \\
L_{vert} &= m_l^2 (x+y) (1-x-y) - m_i^2 (x+y) + m_Z^2 x y, \\
L_{1vert} &= \left(m_l^2 (x+y) - m_i^2 \right) (1-x-y) + m_Z^2 x (y-1), \\
L_{2vert} &= \left(m_l^2 (x+y) - m_i^2 \right) (1-x-y) + m_Z^2 y (x-1), \tag{16}
\end{aligned}$$

and

$$\begin{aligned}
c_{self} &= -\frac{e A_{d_u}}{2 \sin(d_u \pi) \Lambda_u^{2(d_u-1)}}, \\
c_{ver} &= -\frac{e A_{d_u}}{2 s_W c_W \sin(d_u \pi) \Lambda_u^{2(d_u-1)}}, \\
b_{ver} &= -\frac{e A_{d_u}}{2 s_W c_W \sin(d_u \pi) \Lambda_u^{2d_u-1}}, \\
b'_{ver} &= -b_{ver}. \tag{17}
\end{aligned}$$

In eq. (15), the flavor diagonal and flavor changing scalar and pseudoscalar couplings $\lambda_{il}^{S,P}$ represent the effective interaction between the internal lepton i , ($i = e, \mu, \tau$) and the outgoing

l^- (l^+) lepton (anti lepton). Finally, using the form factors f_V , f_A , f_M and f_E , the BR for $Z \rightarrow l^- l^+$ decay is obtained as

$$BR(Z \rightarrow l^+ l^-) = \frac{1}{48\pi} \frac{m_Z}{\Gamma_Z} \{ |f_V|^2 + |f_A|^2 + \frac{1}{2c_W^2} (|f_M|^2 + |f_E|^2) \}, \quad (18)$$

where Γ_Z is the total decay width of Z boson.

Discussion

This section is devoted to the scalar unparticle effect on the BRs of LFC Z boson decays. LFC Z boson decays exist in the tree level in the framework of the SM and there are discrepancies between the SM BRs and the experimental ones. Here, we include the possible scalar unparticle contribution, which appears at least in the one loop, and search whether these contributions could explain the discrepancies in the BRs. We also study the new free parameters which appear with the inclusion of scalar unparticle contribution: the scaling dimension d_u , the new couplings, the energy scale. These parameters should be restricted by respecting the current experimental measurements and some theoretical considerations. First, we choose the scaling dimension d_u in the range³ $1 < d_u < 2$. The scalar unparticles appear in the loops with the following new couplings in the framework of the effective theory: the $U-l-l$ couplings λ_{ij} , the $U-Z-Z$ couplings λ_0 , λ_Z (see eqs. (4, 5) and Fig. 1). For the $U-l-l$ couplings we consider that the diagonal ones λ_{ii} are aware of flavor, $\lambda_{\tau\tau} > \lambda_{\mu\mu} > \lambda_{ee}$ and the off diagonal couplings λ_{ij} are flavor blind, $\lambda_{ij} = \kappa \lambda_{ee}$ with $\kappa < 1$. In our numerical calculations, we choose $\kappa = 0.5$. On the other hand, the possible tree level $U-Z-Z$ interaction (see eqs. (5)) is induced by new couplings λ_0 and λ_Z (see eq. (5)) and, for these couplings, we choose the range $0.1 - 1.0$. Finally, we take the energy scale of the order of TeV. Notice that throughout our calculations we use the input values given in Table (1).

Fig. 2 represents the BR ($Z \rightarrow e^+ e^-$) with respect to the scale parameter d_u , for the couplings $\lambda_{\mu\mu} = 0.1$, $\lambda_{\tau\tau} = 1$, $\lambda_{ij} = 0.5 \lambda_{ee}$, $i \neq j$ and $\lambda_0 = \lambda_Z = 0.1$. Here the solid (dashed) straight line represents the QED corrected SM (the experimental⁴) BR. On the other hand the left-right solid⁵ (dashed, short dashed) curves represent the BR including the scalar unparticle

³Here, $d_u > 1$ is due to the non-integrable singularities in the decay rate [21] and $d_u < 2$ is due to the convergence of the integrals [23].

⁴For the experimental values of the BRs we use the numerical values which are obtained by adding the experimental uncertainties to the mean values.

⁵The solid lines almost coincide.

| Parameter | Value |
|-----------------------------------|--------------|
| m_e | 0.0005 (GeV) |
| m_μ | 0.106 (GeV) |
| m_τ | 1.780 (GeV) |
| Γ_Z^{Tot} | 2.49 (GeV) |
| s_W^2 | 0.23 |
| α_{EM} | 1/129 |
| $BR_{SM}(Z \rightarrow ee)$ | 0.03346 |
| $BR_{SM}(Z \rightarrow \mu\mu)$ | 0.03346 |
| $BR_{SM}(Z \rightarrow \tau\tau)$ | 0.03338 |

Table 1: The values of the input parameters used in the numerical calculations.

contribution, for the energy scale $\Lambda_u = 10\text{ TeV}$ - $\Lambda_u = 1.0\text{ TeV}$, $\lambda_{ee} = 0.01$ (0.05, 0.1). The BR is sensitive to the scale d_u for its values near to one and the experimental result is obtained in the case that the parameter d_u has the values $d_u \leq 1.02$, for the numerical values of the coupling $\lambda_{ee} \sim 0.1$. The scalar unparticle contribution to the BR is negligible for larger d_u values.

Fig. 3 shows the BR ($Z \rightarrow \mu^+ \mu^-$) with respect to the scale parameter d_u , for the couplings $\lambda_{ee} = 0.01$, $\lambda_{\tau\tau} = 1$, $\lambda_{ij} = 0.005$, $i \neq j$ and $\lambda_0 = \lambda_Z = 0.1$. Here the solid (dashed) straight line represents the QED corrected SM (the experimental) BR and the left-right solid⁶ (dashed, short dashed) curves represent the BR including the scalar unparticle contribution, for the energy scale $\Lambda_u = 10\text{ TeV}$ - $\Lambda_u = 1.0\text{ TeV}$ $\lambda_{\mu\mu} = 0.1$ (0.5, 1.0). Similar to the $Z \rightarrow e^+ e^-$ decay the BR is sensitive to the scale d_u for its values near to one and the experimental result is obtained for the range of the parameter d_u , $d_u \leq 1.15$, for the numerical values of the coupling $\lambda_{\mu\mu} \sim 1.0$. The BR is not sensitive the scalar unparticle contribution for larger values of d_u .

In Fig. 4, we present the BR ($Z \rightarrow \tau^+ \tau^-$) with respect to the scale parameter d_u , for the couplings $\lambda_{ee} = 0.01$, $\lambda_{\mu\mu} = 0.1$, $\lambda_{ij} = 0.005$, $i \neq j$ and $\lambda_0 = \lambda_Z = 0.1$. Here the solid (dashed) straight line represents the QED corrected SM (the experimental) BR and the left-right solid (dashed, short dashed) curves represent the BR including the scalar unparticle contribution, for the energy scale $\Lambda_u = 10\text{ TeV}$ - $\Lambda_u = 1.0\text{ TeV}$ $\lambda_{\tau\tau} = 1.0$ (5.0, 10). The addition of the scalar unparticle effect causes that the BR reaches to the experimental result for $d_u \leq 1.25$. It is observed that the scalar unparticle effect results in that the BR becomes smaller than the SM result for the range $1.25 \leq d_u \leq 1.70$. This is due to the mixing terms of the SM and the unparticle contributions.

In Figs. 5 (6, 7) we present the BR ($Z \rightarrow e^+ e^-$) (BR ($Z \rightarrow \mu^+ \mu^-$), BR ($Z \rightarrow \tau^+ \tau^-$)) with

⁶The solid lines almost coincide.

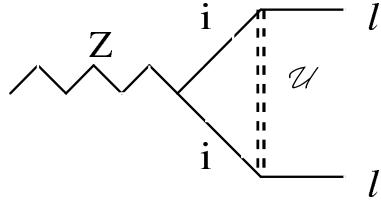
respect to the couplings λ , for different values of the scale parameter d_u . Here the solid (dashed) straight line represents the QED corrected SM (the experimental) BR. In Fig.5 the lower-upper solid (dashed) curves represent the BR with respect to $\lambda = \lambda_{ee}$ where $\lambda_{\mu\mu} = 10\lambda$, $\lambda_{\tau\tau} = 100\lambda$, $\lambda_{ij} = 0.5\lambda$, $\lambda_0 = \lambda_Z = 10\lambda$, for $\Lambda_u = 10\text{ TeV}$ - $\Lambda_u = 1.0\text{ TeV}$, $d_u = 1.01$ ($d_u = 1.1$). It is observed that the experimental result is reached for the numerical values of the scale parameter d_u not greater than ~ 1.01 for the coupling $\lambda > 0.065$. In Fig.6 the lower-upper solid (the lower-upper dashed, the lower-upper short dashed) curves represents the BR with respect to $\lambda = \lambda_{\mu\mu}$ where $\lambda_{ee} = 0.1\lambda$, $\lambda_{\tau\tau} = 10\lambda$, $\lambda_{ij} = 0.05\lambda$, $\lambda_0 = \lambda_Z = \lambda$, for $\Lambda_u = 10\text{ TeV}$ - $\Lambda_u = 1.0\text{ TeV}$ $d_u = 1.1$ ($\Lambda_u = 10\text{ TeV}$ - $\Lambda_u = 1.0\text{ TeV}$ $d_u = 1.2$, $\Lambda_u = 1.0\text{ TeV}$ - $\Lambda_u = 10\text{ TeV}$ $d_u = 1.3$). The experimental result is obtained for $d_u \sim 1.1$ and for the coupling $\lambda > 0.5$ in the case that the energy scale is of the order of $\Lambda_u = 1.0\text{ TeV}$. In Fig.7 the lower-upper solid (the lower-upper dashed, the lower-upper short dashed) curves represent the BR with respect to $\lambda = \lambda_{\tau\tau}$ where $\lambda_{ee} = 0.01\lambda$, $\lambda_{\mu\mu} = 0.1\lambda$, $\lambda_{ij} = 0.005\lambda$, $\lambda_0 = \lambda_Z = 0.1\lambda$, for $\Lambda_u = 10\text{ TeV}$ - $\Lambda_u = 1.0\text{ TeV}$ $d_u = 1.1$ ($\Lambda_u = 10\text{ TeV}$ - $\Lambda_u = 1.0\text{ TeV}$ $d_u = 1.2$, $\Lambda_u = 1.0\text{ TeV}$ - $\Lambda_u = 10\text{ TeV}$ $d_u = 1.3$). In this decay the experimental result is obtained for $d_u \sim 1.2$ and for the coupling $\lambda > 2.5$ in the case that the energy scale is of the order of $\Lambda_u = 1.0\text{ TeV}$. For $d_u \sim 1.1$ the experimental result is reached even for small couplings, $\lambda < 1.0$.

As a summary, the LFC Z boson decays are sensitive to the unparticle scaling dimension d_u for its small values. The experimental result of the BR is obtained for the parameter $d_u < 1.2$ for heavy lepton flavor output and the discrepancy between QED corrected SM result and the experimental one can be explained by the scalar unparticle effect. This may be a clue for the existence of unparticles and informative in the determination of the scaling parameter d_u . For light flavor output one needs to choose the parameter d_u near to one and, for the values of d_u which are slightly far from one, the discrepancy between QED corrected SM result and the experimental can not be explained by the unparticle contribution. Therefore, with the forthcoming more accurate measurements of the decays under consideration, especially the one with heavy lepton flavor output, it would be possible to test the possible signals coming from the unparticle physics

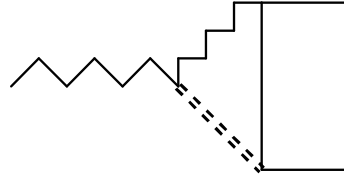
References

- [1] R. Hawkins and K. Mönig, *Eur. Phys. J. direct* **C8** (1999) 1.
- [2] W. M. Yao, et.al, *J. Phys.* **G33** (2006) 1.
- [3] CDF Collaboration, (T. Kamon for the collaboration). FERMILAB-CONF-89/246-E, Dec 1989. 25pp. To be publ. in Proc. of 8th Topical Workshop on p anti-p Collider Physics, Castiglione d. Pescaia, Italy, Sep 1-5, 1989. Published in Pisa Collider Workshop 1989:0281-305 (QCD161:W64:1989).
- [4] ALEPH Collaboration, D. Decamp *et al.*, *Phys.Lett.* **B263** 112 (1991).
- [5] ALEPH Collaboration, D. Decamp *et al.*, *Phys.Lett.* **B265** 430 (1991).
- [6] W. Bernreuther, G.W. Botz, O. Nachtmann, P. Overmann, *Z.Phys.* **C52** 567 (1991).
- [7] DELPHI Collaboration, P. Abreu *et al.*, *Z. Phys.* **C55** 555 (1992).
- [8] LEP Collaboration, *Phys. Lett.* **B276** 247 (1992).
- [9] OPAL Collaboration, P. D. Acton *et al.*, *Phys. Lett.* **B281** 405 (1992).
- [10] ALEPH Collaboration, D. Buskulic *et al.*, *Phys.Lett.* **B297** 459 (1992).
- [11] U. Stiegler, *Z. Phys.* **C58** 601 (1993).
- [12] ALEPH Collaboration, D. Buskulic *et al.*, *Z. Phys.* **C59** 369 (1993).
- [13] U. Stiegler, *Z. Phys.* **C57** 511 (1993).
- [14] J. Bernabeu, G.A. Gonzalez-Sprinberg, J. Vidal *Phys. Lett.* **B326** 168 (1994).
- [15] F. Sanchez, *Phys. Lett.* **B384** 277 (1996).
- [16] A. Posthaus, P. Overmann, *JHEP* **9802:001** (1998).
- [17] E. Iltan, *Phys. Rev.* **D65** 036003 (2002).
- [18] E. Iltan, *Phys. Rev.* **D66** 034011 (2002).
- [19] M. I. Vysotsky, V. A. Novikov, L. B. Okun, A. N. Rozanov, *Phys. Usp.* **39** 503 (1996).
- [20] H. Georgi, *Phys. Rev. Lett.* **98**, 221601 (2007).

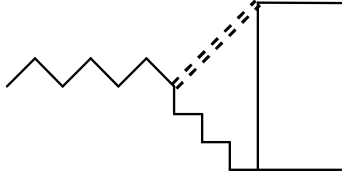
- [21] H. Georgi, *Phys. Lett.* **B650**, 275 (2007).
- [22] C. D. Lu, W. Wang and Y. M. Wang, *Phys.Rev.* **D76**, 077701 (2007).
- [23] Y. Liao, *Phys. Rev.* **D76**, 056006 (2007).
- [24] K. Cheung, W. Y. Keung and T. C. Yuan, *Phys. Rev.* **D76**, 055003 (2007).
- [25] D. Choudhury and D. K. Ghosh, hep-ph/0707.2074 (2007).
- [26] G. J. Ding and M. L. Yan, *Phys. Rev.* **D77**, 014005 (2008).
- [27] Y. Liao, hep-ph/0708.3327 (2007).
- [28] K. Cheung, T. W. Kephart, W. Y. Keung and T. C. Yuan, hep-ph/0801.1762 (2008).
- [29] E. O. Iltan, hep-ph/0710.2677 (2007).
- [30] E. O. Iltan, hep-ph/0711.2744 (2007).
- [31] E. O. Iltan, hep-ph/0802.1277 (2008).
- [32] R. Zwicky, hep-ph/0707.0677 (2007).
- [33] S. L. Chen and X. G. He, *Phys. Rev.* **D76**, 091702 (2007).
- [34] K. Cheung, W. Y. Keung and T. C. Yuan, *Phys. Rev. Lett.* **99**, 051803 (2007).



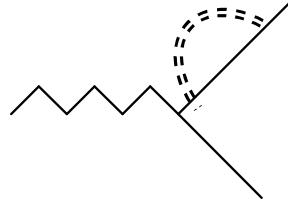
(a)



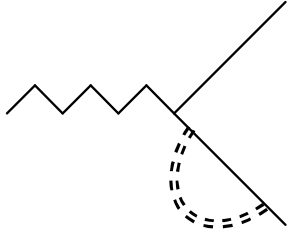
(b)



(c)



(d)



(e)

Figure 1: One loop diagrams contribute to $Z \rightarrow l^+ l^-$ decay with scalar unparticle mediator. Solid line represents the lepton field: i represents the internal lepton, l^- (l^+) outgoing lepton (anti lepton), wavy line the Z boson field, double dashed line the unparticle field.

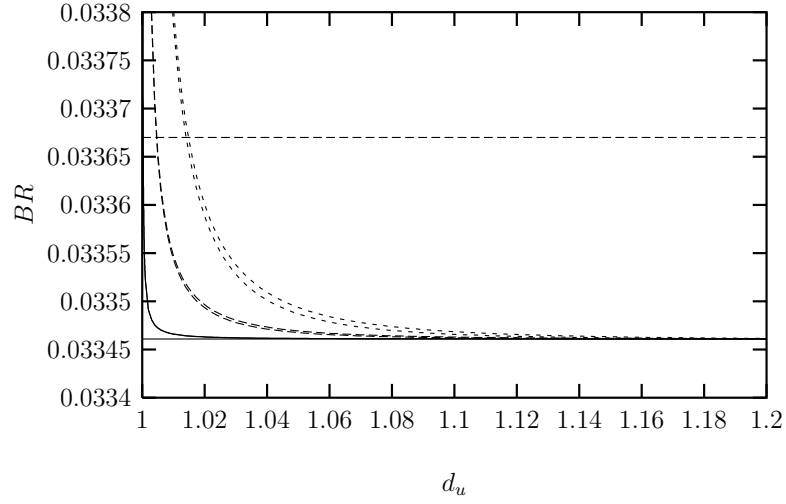


Figure 2: The scale parameter d_u dependence of the BR ($Z \rightarrow e^+ e^-$) for $\Lambda_u = 10 \text{ TeV}$, $\lambda_{ee} = 0.01$, $\lambda_{\mu\mu} = 0.1$, $\lambda_{\tau\tau} = 1$, $\lambda_{ij} = 0.005$, $i \neq j$ and $\lambda_0 = \lambda_Z = 0.1$. The solid (dashed) straight line represents the SM (experimental) BR and the left-right solid (dashed, short dashed) curves represent the BR including the scalar unparticle contribution, for the energy scale $\Lambda_u = 10 \text{ TeV}$ - $\Lambda_u = 1.0 \text{ TeV}$ $\lambda_e = 0.01$ (0.05, 0.1).

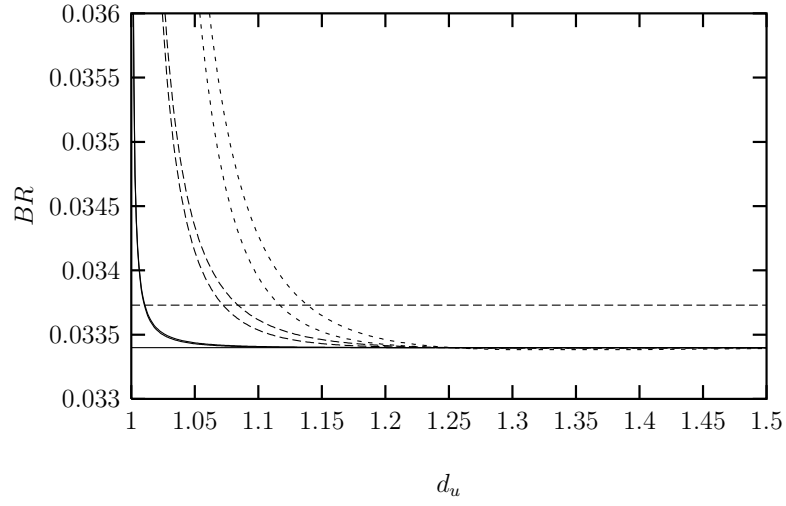


Figure 3: The scale parameter d_u dependence of the BR ($Z \rightarrow \mu^+ \mu^-$) for $\lambda_{ee} = 0.01$, $\lambda_{\tau\tau} = 1$, $\lambda_{ij} = 0.005$, $i \neq j$ and $\lambda_0 = \lambda_Z = 0.1$. The solid (dashed) straight line represents the SM (experimental) BR and the left-right solid (dashed, short dashed) curves represent the BR including the scalar unparticle contribution, for the energy scale $\Lambda_u = 10 \text{ TeV}$ - $\Lambda_u = 1.0 \text{ TeV}$ $\lambda_{\mu\mu} = 0.1$ (0.5, 1.0).

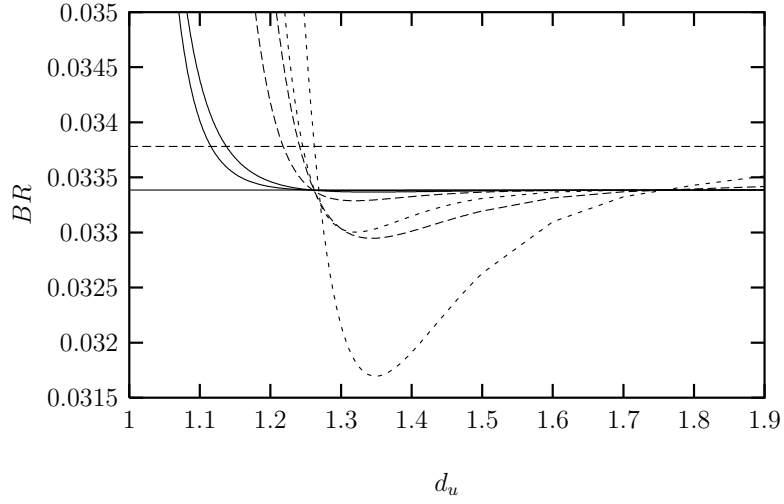


Figure 4: The scale parameter d_u dependence of the BR ($Z \rightarrow \tau^+ \tau^-$) for $\lambda_{ee} = 0.01$, $\lambda_{\mu\mu} = 0.1$, $\lambda_{ij} = 0.005$, $i \neq j$ and $\lambda_0 = \lambda_Z = 0.1$. The solid (dashed) straight line represents the SM (experimental) BR and the left-right solid (dashed, short dashed) curves represent the BR including the scalar unparticle contribution, for the energy scale $\Lambda_u = 10 \text{ TeV}$ - $\Lambda_u = 1.0 \text{ TeV}$ $\lambda_{\tau\tau} = 1.0$ (5.0, 10).

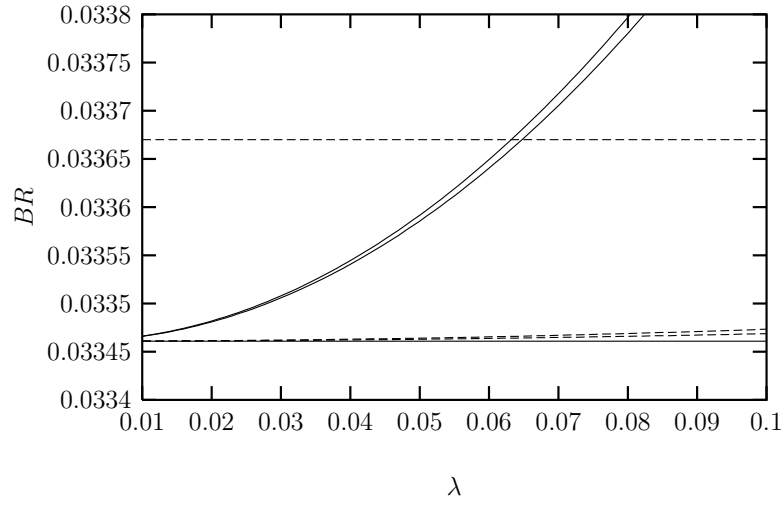


Figure 5: The coupling λ dependence of the BR ($Z \rightarrow e^+ e^-$). The solid (dashed) straight line represents the SM (experimental) BR and the lower-upper solid (dashed) curve represents the BR with respect to $\lambda = \lambda_{ee}$ where $\lambda_{\mu\mu} = 10 \lambda$, $\lambda_{\tau\tau} = 100 \lambda$, $\lambda_{ij} = 0.5 \lambda$, $\lambda_0 = \lambda_Z = 10 \lambda$, for $\Lambda_u = 10 \text{ TeV}$ - $\Lambda_u = 1.0 \text{ TeV}$ $d_u = 1.01$ ($d_u = 1.1$) .

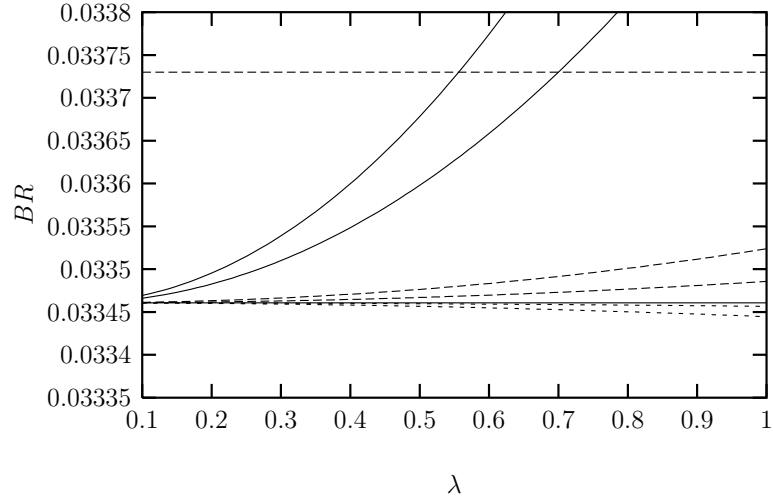


Figure 6: The coupling λ dependence of the BR ($Z \rightarrow \mu^+ \mu^-$). The solid (dashed) straight line represents the SM (experimental) BR and the lower-upper solid (the lower-upper dashed, the lower-upper short dashed) curve represents the BR with respect to $\lambda = \lambda_{\mu\mu}$ where $\lambda_{ee} = 0.1 \lambda$, $\lambda_{\tau\tau} = 10 \lambda$, $\lambda_{ij} = 0.05 \lambda$, $\lambda_0 = \lambda_Z = \lambda$, for $\Lambda_u = 10 \text{ TeV}$ - $\Lambda_u = 1.0 \text{ TeV}$ $d_u = 1.1$ ($\Lambda_u = 10 \text{ TeV}$ - $\Lambda_u = 1.0 \text{ TeV}$ $d_u = 1.2$, $\Lambda_u = 1.0 \text{ TeV}$ - $\Lambda_u = 10 \text{ TeV}$ $d_u = 1.3$) .

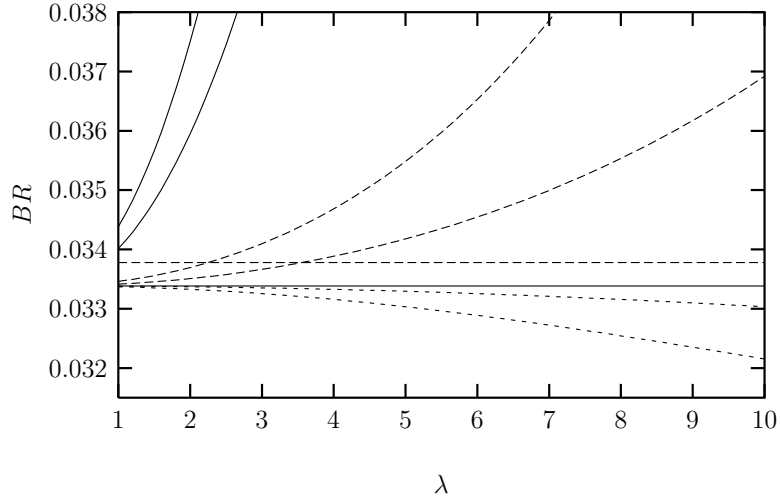


Figure 7: The coupling λ dependence of the BR ($Z \rightarrow \tau^+ \tau^-$). The solid (dashed) straight line represents the SM (experimental) BR and the lower-upper solid (the lower-upper dashed, the lower-upper short dashed) curve represents the BR with respect to $\lambda = \lambda_{\tau\tau}$ where $\lambda_{ee} = 0.01 \lambda$, $\lambda_{\mu\mu} = 0.1 \lambda$, $\lambda_{ij} = 0.005 \lambda$, $\lambda_0 = 0.1 \lambda$, for $\Lambda_u = 10 \text{ TeV}$ - $\Lambda_u = 1.0 \text{ TeV}$ $d_u = 1.1$ ($\Lambda_u = 10 \text{ TeV}$ - $\Lambda_u = 1.0 \text{ TeV}$ $d_u = 1.2$, $\Lambda_u = 1.0 \text{ TeV}$ - $\Lambda_u = 10 \text{ TeV}$ $d_u = 1.3$) .